



A modified Damascene electrodeposition process for bottom-up filling of recessed surface features

Chang Hwa Lee, Thomas P. Moffat*

Materials Science and Engineering Laboratory, National Institute of Standards and Technology, Gaithersburg, MD 20899, USA

ARTICLE INFO

Article history:

Received 6 April 2010

Received in revised form 9 July 2010

Accepted 17 July 2010

Available online 23 July 2010

Keywords:

Damascene process

Nickel

Superconformal deposition

Bottom-up filling

Mercaptobenzimidazole

ABSTRACT

A modification of the conventional Damascene metallization process is described whereby selective removal of the thin wetting/seed layer from the sidewalls and free surfaces enables selective nucleation and bottom-up electrodeposition of metals and alloys in recessed surface features. The process is demonstrated by filling sub-micrometer trenches with electrodeposited Ni. A conventional PVD Cu seed layer is etched to remove Cu from the sidewalls and free surface while leaving a continuous Cu wetting layer intact on the trench bottom. The underlying non-wetting barrier layer provides a conductive path for electrodeposition from contacts on the perimeter of the work piece to the trench bottom. The robustness of the bottom-up Ni electrodeposition process is greatly increased by the addition of 2-mercaptobenzimidazole (MBI) to the plating bath. The additive hinders spurious nucleation of Ni on residual Cu patches that may remain on the free surface.

Published by Elsevier Ltd.

1. Introduction

The realization of three-dimensional (3D) metal structures has become a central theme in the densification of microelectronics and energy conversion devices ranging from through-silicon-vias (TSV) and micro-electro-mechanical systems (MEMS) to battery electrodes and the metallization of photovoltaic devices [1–8].

Conventional 2D (or 2.5D) processes, such as through-mask plating, templated deposition, or LIGA (lithography, electroplating, and molding), have been utilized to manufacture patterned microstructures made of iron group metals, Ni, Co, Fe and alloys thereof, for use in magnetic recording heads, sensors, MEMS, etc. [6–13]. A typical process involves metal electrodeposition on a conductive substrate that is masked by a non-conducting patterned photoresist or a porous oxide template that guides the vertical growth of the metal deposit. Although this has proven to be a very powerful fabrication method, there are serious constraints to building complex multilayered 3D metal structures. For example, electrical addressability is required for the electrodeposition process, but some device designs might call for electrical isolation of individual segments during subsequent processing steps. The latter curtails the ability to build complex 3D structures. In contrast, the Damascene process that has been widely used in building Cu interconnects [14,15] offers an efficient way to build complex

multilayered 3D structures without the need to maintain electrical continuity between subsequent layers. The conventional Cu Damascene process relies on additive-derived superconformal metal electrodeposition to robustly fill trenches and vias on metallized surfaces. Competitive interactions between inhibiting and accelerating adsorbates convoluted with area change enable void-free superconformal filling of recessed features. The same deposition mechanism has also been shown to be applicable to other passive interconnect materials such as Ag and Au [16–18]. More recently, the prospect of designing and building active, functional materials in 3D metallized structures has received attention and reports of superconformal electrodeposition of Ni and related iron-group magnetic alloys are available [19–22]. Addition of a single additive, such as the mercaptobenzimidazole derivatives, MBIS and MBI [20,21], or polymers such as polyethyleneimine [19], to an additive-free Ni plating bath has been shown to be effective in generating void-free trench filling by a mechanism that is distinct from that used for the Group IB metals [15–18]. The feature filling involves an inhibition-breakdown process that initially gives rise to a v-notch shaped growth front within the trench followed by geometric leveling. Two challenges to practical implementation of the process remain. Firstly, the plated overburden tends to vary with feature size, which hampers subsequent CMP processing. Secondly, in some instances the superconformal growth dynamic is unable to compensate for non-uniformities associated with physical vapor deposited (PVD) Cu seed layers. For example, reentrant sidewall angles associated with Cu seed layer build up and overhang at the trench mouth can lead to center and top voids in the final plated structure that is especially evident in narrow features [21].

* Corresponding author. Tel.: +1 301 975 2143; fax: +1 301 926 7679.
E-mail address: thomas.moffat@nist.gov (T.P. Moffat).

More recently, attempts have been made to selectively poison or prevent electrodeposition on the conductive free surface in order to optimize, and potentially simplify, the Damascene process flow. Techniques ranging from PVD of a non-wetting Ta layer [23] to derivatization of the free surface with alkane thiol films [12,13,24] have been shown to selectively block metal deposition reactions. Likewise, processes that couple mechanical and chemical action to minimize deposition on the free surface, relative to recessed features, have also been explored [25]. Most recently, a mixed-mode Damascene like-variation of through-mask deposition has been explored [22]. This process involved selective etching to remove all conductive materials from the free surface of the trench-patterned substrate followed by electroplating where current was directed to the trenches via a common back contact in a manner congruent with traditional through-mask plating. The remaining metallized sidewalls and trench bottom resulted in superconformal feature filling. A significant limitation of this scheme is that the entire structure remains electrically connected via the original back plane contact. In principle, the back plane of a single layer structure could be removed to electrically isolate individual features. However, it is not obvious how this process could be extended to build the intricate multilayered 3D structures.

In this paper we introduce another mixed-mode deposition process whereby the advantages of 3D electrical addressability associated with Damascene processing are coupled with the bottom-up feature filling dynamic typically associated with through-mask processing. This is accomplished by selectively removing the wetting Cu seed layer from the free surface and trench sidewalls while leaving the conductive barrier layer intact across the topographically patterned work piece. The Cu seed layer that remains on the bottom surface of the recessed features serves as a site for electrodeposition while the non-wetting sidewalls provide an electrical conduction pathway as well as templating for bottom-up feature filling. The bottom-up growth mode also offers the prospect of controlling the orientation of the deposited material by appropriate consideration of the barrier/seed layer architecture. The properties of the interface formed between the electrodeposits and the “non-wetting” sidewalls remain to be investigated. Partial oxidation of the barrier layer during etching and transfer to the plating bath is likely however conventional barriers are thick enough to ensure suitable conductivity remains. The robustness of the filling process is dependent on nucleation being restricted to the bottom surface of the metallized trench. This is accomplished by addition of an inhibitor to the plating electrolyte to block sporadic nucleation and growth of material on the free surface between trenches. This strategy is analogous to that recently used in the formulation of

defect tolerant directional etch systems based on monolayer resists [26].

2. Experimental

The substrates used for this study consist of a PVD Cu seed layer over a Ta barrier layer deposited on Si wafers that were lithographically patterned with trench arrays with various feature widths. Ni deposition was performed under potentiostatic conditions using a three-electrode cell, with a Pt wire anode and a saturated calomel reference electrode (SCE). A Watts-type bath consisting of $1.0 \text{ mol L}^{-1} \text{ NiSO}_4 \cdot 6\text{H}_2\text{O}$, $0.2 \text{ mol L}^{-1} \text{ NiCl}_2 \cdot 6\text{H}_2\text{O}$, and $0.5 \text{ mol L}^{-1} \text{ H}_3\text{BO}_3$ (pH 3.4) was used in both the absence and presence of $150 \mu\text{mol L}^{-1}$ 2-mercaptobenzimidazole (MBI). Selective etching to remove the Cu seed layer from the free-surface and trench sidewalls was performed by immersing the substrates in a mixture of 0.02 mol L^{-1} citric acid and 0.2 mol L^{-1} (2 wt%) H_2O_2 (pH 4) for 4 min prior to the metal deposition process. The citric acid and H_2O_2 are well-known as a complexing agent and oxidizer, respectively. The combination has been effectively used for chemical mechanical polishing (CMP) of Cu [27,28]. Following etching, the specimens were rinsed with $18 \text{ M}\Omega \text{ cm}$ DI water, dried with N_2 gas flow, and then immediately immersed into the plating bath with the potential applied. Cleaved cross-sections of the Ni filled trenches were examined using a field emission scanning electron microscopy (FE-SEM). Irregular morphologies are apparent in some cross-section images. These are simply artifacts of the specimen cleavage process that leads to ductile tearing of the electrodeposited Ni and fracture of the interfaces between the Ni and the Cu/Ta under-layers.

3. Results and discussion

FE-SEM images of cross-sectioned Cu seeded trench arrays prior to Cu seed removal and Ni deposition are shown in Fig. 1. The trench widths range from 150 nm to 2200 nm. Inspection reveals significant differences in the Cu film thickness on the top, bottom and sidewalls of the trenches. For the larger features examined, TEM analysis (not shown) reveals 25 nm of Ta and 120 nm of Cu on the horizontal surfaces (i.e. free surface and trench bottom) while the sidewalls are covered with only 5 nm Ta and 10 nm Cu. The difference between the horizontal and vertical surfaces is a consequence of the line-of-sight nature of the PVD process. This leads to significant lateral growth on concave features evident by the significant “overhang” of the Cu seed layer at the top corners of the trenches with the corresponding reduction of thickness at the shadowed bottom corners. The reentrant nature of the upper sidewall geometry

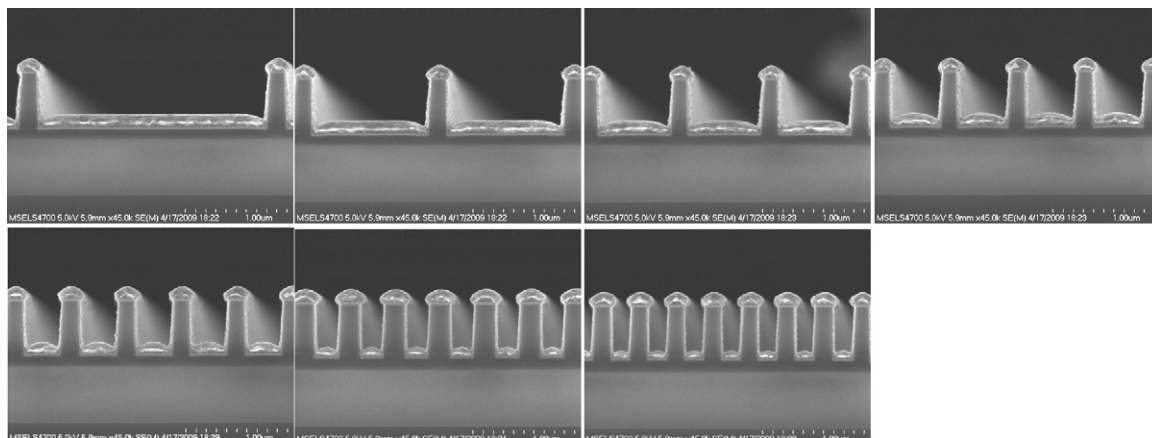


Fig. 1. Cross-section of Cu seeded trench arrays. Note the thin sidewall coverage, build-up and overhang on the top corners of the trenches.

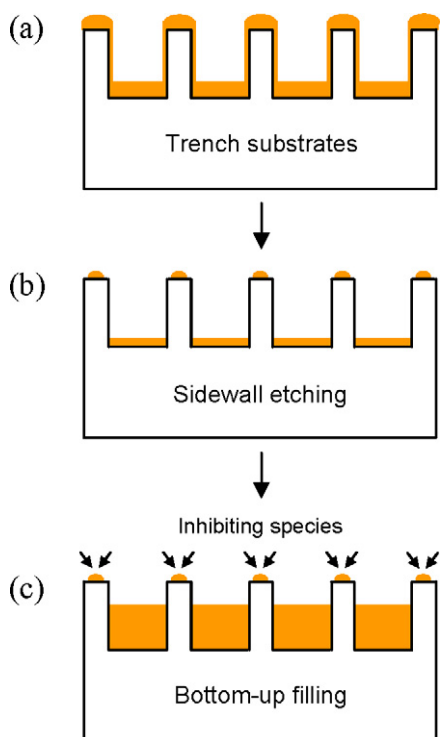


Fig. 2. Schematic diagram of a modified Damascene processes that uses controlled nucleation and substrate topography to guide a bottom-up electrodeposition process.

represents a challenge to subsequent feature filling and effectively narrows the processing window, thereby increasing the likelihood of undesired void formation during subsequent feature filling by electrodeposition. For a given seed layer thickness the negative effect is increasingly severe for narrower features.

Additive-free Ni deposition on such seed layers results in a continuous center-line void that forms following collision of the opposing sidewalls that grow conformally from the top corners of the trench. In contrast, Ni deposition in the presence of inhibitors, such as PEI, MBIS and MBI, has been shown to result in transient inhibition of the metal deposition on the upper corners that makes void-free filling of sub-micrometer features possible [19–21].

As an alternative to the conventional Damascene process, the scheme shown in Fig. 2 is explored herein. Etching time was controlled to selectively remove the Cu seed layer from the sidewalls and free surface while leaving Cu on the bottom trench surface

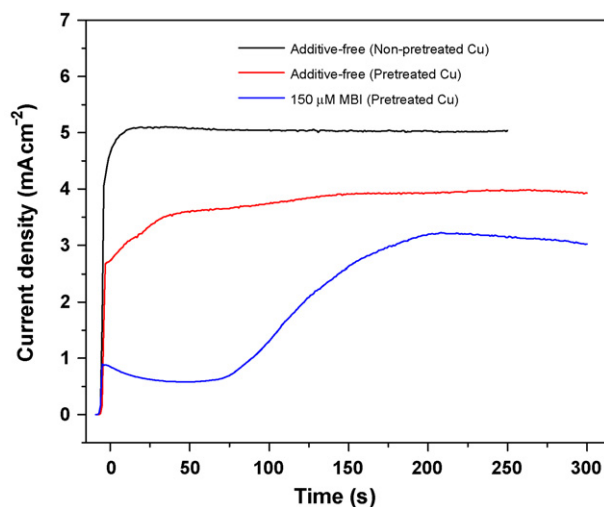


Fig. 4. Current transients at -0.9 V SCE for Ni electrodeposition (a) on a Cu seeded substrate in an additive-free plating electrolyte, (b) a selectively etched substrates in an additive-free plating electrolyte, (c) a selectively etched substrates in an electrolyte containing $150 \mu\text{mol L}^{-1}$ MBI.

to facilitate selective nucleation during subsequent Ni electroplating. The Cu seeded specimens were etched for 4 min in a mixture of 0.02 mol L^{-1} citrate and 0.2 mol L^{-1} H_2O_2 . The PVD derived thickness variations naturally lead to rapid loss of Cu from the sidewalls. The relative accessibility of the free surface compared to the recessed trench bottom provides an avenue for development of a differential, topographically dependent etch rate between the respective surfaces. Following etching the specimens were rinsed with DI water and transferred into an additive-free Ni plating bath at -0.9 V SCE for 300 s for Ni plating. As shown in Fig. 3 in the wider (e.g. 680 nm) trenches Ni is exclusively deposited on the bottom surface. In contrast, significant Ni deposition is evident on the free surfaces neighboring the finer (460 nm down to 150 nm) trenches. This is attributed to some residual amount of the Cu seed layer still present on the free surface. The remnant Cu seed on the free surface is the result of the similar thickness of the original Cu seed layer and trench bottom combined with the effect of pattern density on etchant depletion. In principle this effect may be circumvented in a number of ways. Stronger feature height dependent etching might be induced by coupling the existing chemistry with a hydrodynamic shear motion in a manner analogous to conventional chemical mechanical planarization process. Furthermore, modification of the etching chemistry with

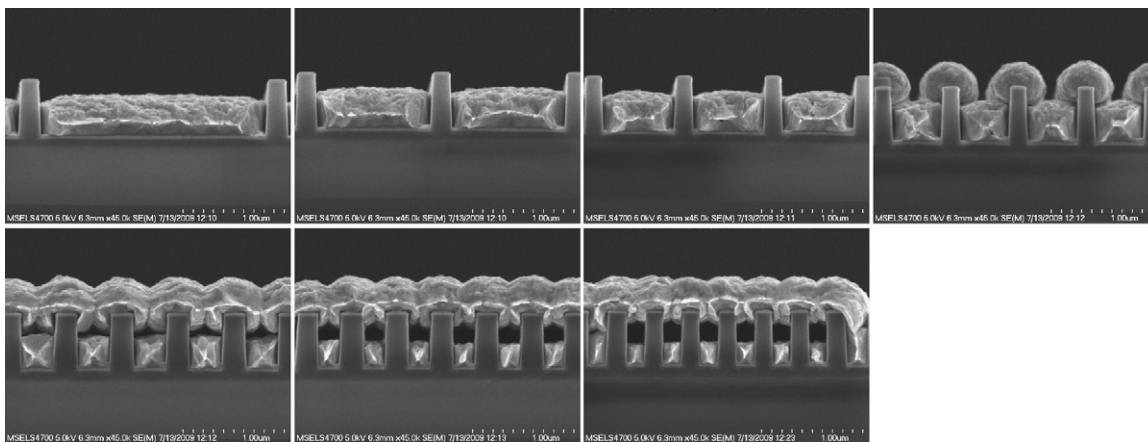


Fig. 3. Ni electrodeposition on Cu seeded trench patterned substrates that have been etched to remove Cu from the sidewalls and top surface. Ni deposition was performed in an additive-free solution at a growth potential of -0.9 V SCE for 300 s.

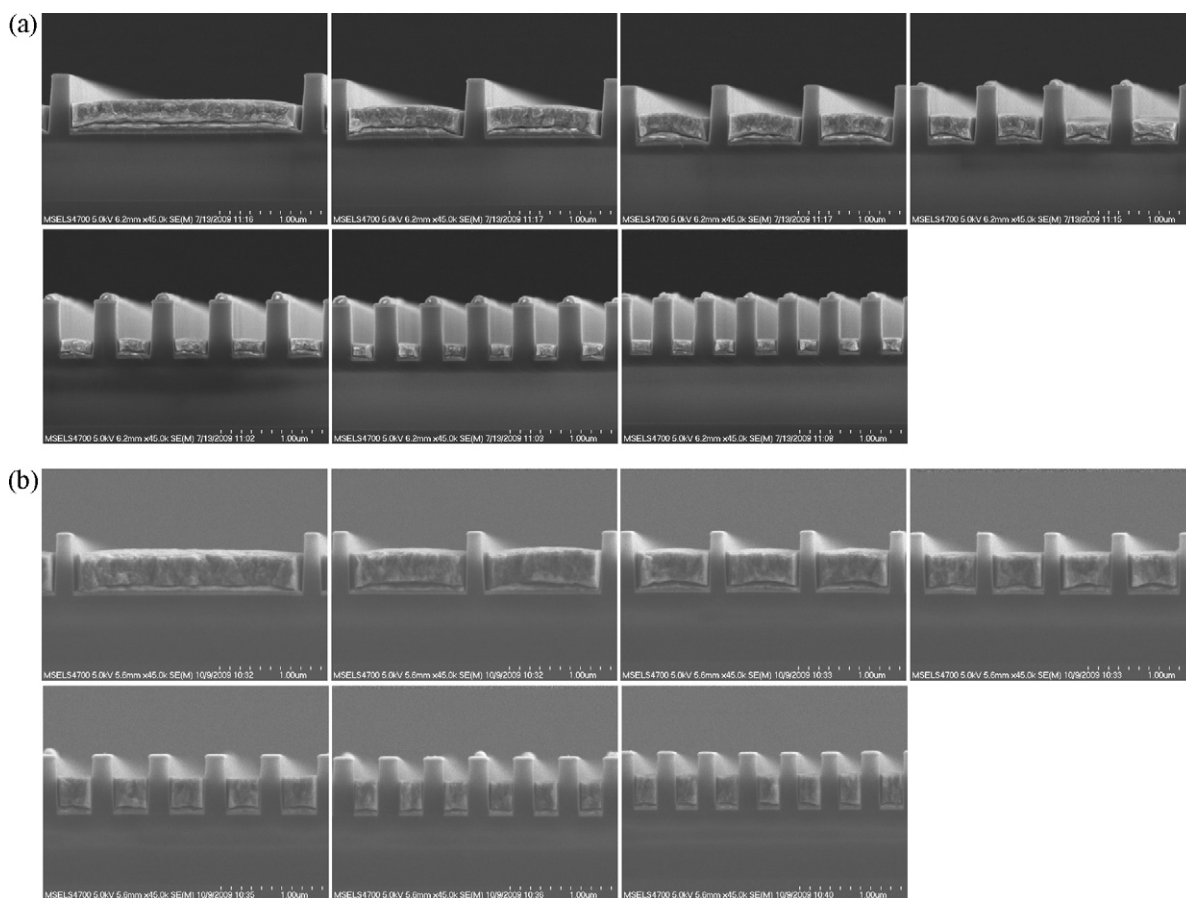


Fig. 5. Ni electrodeposition on Cu seeded trench patterned substrates that have been etched to remove Cu from the sidewalls and top surface. Ni deposition was performed in a plating electrolyte containing $150 \mu\text{mol L}^{-1}$ MBI at a growth potential of -0.9 V SCE for (a) 300 s and (b) 600 s.

additives might be used to selectively enhance the inhibition of Cu dissolution from the trench bottom during the etching step. Such an approach might require an additional step to remove the inhibitor in order to guarantee effective nucleation of Ni on Cu during the subsequent plating operation. A simpler variant to the above is to use an inhibitor in the Ni electrodeposition process that preferentially interacts with any residual Cu on the free surface to hinder Ni deposition thereon. This approach was explored using MBI additions to the Ni plating bath.

The influence of the etching treatment and MBI additions on the chronoamperometric response associated with Ni deposition on the patterned substrates is shown in Fig. 4. The transient for additive-free Ni deposition on the etched substrate is similar to that for an as-received Cu seeded substrate. The diminished magnitude of the current reflects the loss of electroactive area due to the absence of metal deposition on the etched sidewalls. In the presence of MBI, significant inhibition is evident associated with the formation of a blocking layer that is followed by its subsequent breakdown. The activation process corresponds to autocatalytic breakdown of the inhibiting layer whereby the flux of MBI required to maintain the passive state is overwhelmed by its consumption induced by metal deposition. Similar chronoamperometry has been reported for Ni and Co deposition in the presence of a sulfonated version of the molecule, known as MBIS [20,21].

The combination of selective removal of the Cu seed layer by etching followed by Ni deposition in the presence of MBI leads to very effective bottom-up feature filling. A series of images following 300 s and 600 s of Ni deposition are shown in Fig. 5a and b, respectively. After 300 s, bottom-up Ni deposition by selective deposition

on the Cu seed layer that remains on the trench bottom is unambiguous. Examination of the free surface of the widest trenches indicates that the Cu seed was effectively removed from the free surface. For trench array with feature widths smaller than 400 nm some remnant of the Cu seed layer is clearly evident on the free surface segments between the trenches; However, MBI is remarkably effective in suppressing Ni deposition on these sites compared to the additive-free case (Fig. 3). After 300 s, bottom-up filling has progressed furthest in the widest features. This is in direct contrast to the effect of MBI or MBIS on Ni deposition on continuous Cu seed layers used in the conventional Damascene process [20,21]. At longer deposition times, 600 s, the growth front in the finer feature appears to catch up with bottom-up feature filling evident across trench arrays while negligible deposition occurs on the intervening free-surface areas. A few remnant Cu spots are still evident on the free surface but little Ni deposition has occurred reflecting the effectiveness of MBI. The near uniform growth front across the wide feature sizes may be beneficial to any subsequent CMP process.

Looking to the future, coupling this processing scheme with more complex additive combinations (i.e. accelerators and inhibitors) offers the prospect of further increases in the magnitude of the differential bottom-up growth dynamic.

4. Conclusions

A modified or hybrid Damascene electrodeposition process was demonstrated. Seed layer modification combined with an inhibiting plating additive enables selective nucleation at trench bottoms followed by bottom-up feature filling with growth contours reminiscent of the through-mask plating process. Specifically,

Ni electrodeposition from an MBI containing electrolyte is controlled by selective nucleation on a Cu seed layer that covers only the bottom surface of the trenches thereby enabling exclusive bottom-up feature filling. The MBI plating additives serves to preferentially inhibit Ni deposition on any remnant Cu or other nucleation sites on the free surface, greatly enhancing the robustness of the overall process. Overall, the ability to restrict nucleation to the trench bottoms exploits the short coming of the line-of-sight PVD Cu process. Patterning methods that enable controlled placement, and perhaps texturing, of the nucleating seed layer on top of the non-wetting conductive barrier layer promise new opportunities to design and build heretofore unrealized microstructures.

References

- [1] Z.Y. Fan, H. Razavi, J.W. Do, A. Moriwaki, O. Ergen, Y.L. Chueh, P.W. Leu, J.C. Ho, T. Takahashi, L.A. Reichertz, S. Neale, K. Yu, M. Wu, J.W. Ager, A. Javey, *Nat. Mater.* 8 (2009) 648.
- [2] E. Van Kerschaver, G. Beaucarne, *Prog. Photovoltaics* 14 (2006) 107.
- [3] J.A.D. Jensen, P. Moller, T. Bruton, N. Mason, R. Russell, J. Hadley, P. Verhoeven, A. Matthewson, *J. Electrochem. Soc.* 150 (2003) G49.
- [4] P.H.L. Notten, F. Roozeboom, R.A.H. Niessen, L. Baggetto, *Adv. Mater.* 19 (2007) 4564.
- [5] A.W. Topol, D.C. La Tulipe, L. Shi, D.J. Frank, K. Bernstein, S.E. Steen, A. Kumar, G.U. Singco, A.M. Young, K.W. Guarini, M. Jeong, *IBM J. Res. Dev.* 50 (2006) 491.
- [6] W. Ehrfeld, *Electrochim. Acta* 48 (2003) 2857.
- [7] L.T. Romankiw, *Electrochim. Acta* 42 (1997) 2985.
- [8] J.J. Kelly, N.Y.C. Yang, *Microsyst. Technol.* 11 (2005) 331.
- [9] P.C. Andricacos, N. Robertson, *IBM J. Res. Dev.* 42 (1998) 671.
- [10] O. Azzaroni, P.L. Schilardi, R.C. Salvarezza, *Appl. Phys. Lett.* 80 (2002) 1061.
- [11] T.M. Whitney, J.S. Jiang, P.C. Searson, C.L. Chien, *Science* 261 (1993) 1316.
- [12] T.P. Moffat, H.J. Yang, *J. Electrochem. Soc.* 142 (1995) L220.
- [13] N.S. Pesika, A. Radisic, K.J. Stebbe, P.C. Searson, *Nano Lett.* 6 (2006) 1023.
- [14] P.C. Andricacos, C. Uzoh, J.O. Dukovic, J. Horkans, H. Deligianni, *IBM J. Res. Dev.* 42 (1998) 567.
- [15] T.P. Moffat, D. Wheeler, M.D. Edelstein, D. Josell, *IBM J. Res. Dev.* 49 (2005) 19.
- [16] B.C. Baker, C. Witt, D. Wheeler, D. Josell, T.P. Moffat, *Electrochem. Solid State Lett.* 6 (2003) C67.
- [17] E.J. Ahn, J.J. Kim, *Electrochem. Solid State Lett.* 7 (2004) C118.
- [18] D. Josell, D. Wheeler, T.P. Moffat, *J. Electrochem. Soc.* 153 (2006) C11.
- [19] S.-K. Kim, J.E. Bonevich, D. Josell, T.P. Moffat, *J. Electrochem. Soc.* 154 (2007) D443.
- [20] C.H. Lee, J.E. Bonevich, J.E. Davies, T.P. Moffat, *J. Electrochem. Soc.* 155 (2008) D499.
- [21] C.H. Lee, J.E. Bonevich, J.E. Davies, T.P. Moffat, *J. Electrochem. Soc.* 156 (2009) D301.
- [22] Y. Nakamaru, H. Honma, *Trans. Inst. Met. Finish* 87 (2009) 259.
- [23] O. Luhn, A. Radisic, P.M. Vereecken, C. Van Hoof, W. Ruythooren, J.-P. Celis, *Electrochem. Solid State Lett.* 12 (2009) D39; O. Luhn, A. Radisic, C. Van Hoof, W. Ruythooren, J.-P. Celis, *J. Electrochem. Soc.* 157 (2010) D242.
- [24] S.-K. Kim, J.J. Kim, *Electrochem. Solid State Lett.* 7 (2004) C101.
- [25] B.M. Basol, *J. Electrochem. Soc.* 151 (2004) C765.
- [26] M. Geissler, H. Schmid, A. Boetsch, B. Michel, E. Delamarche, *Langmuir* 18 (2002) 2374.
- [27] M.C. Kang, H.S. Nam, H.Y. Won, S. Jeong, H. Jeong, J.J. Kim, *Electrochem. Solid State Lett.* 11 (2008) H32.
- [28] D.H. Eom, I.K. Kim, J.H. Han, J.G. Park, *J. Electrochem. Soc.* 154 (2007) D38.